R. & M. No. 2263
(6784)
A.R.C. Technical Report

MINISTRY OF SUPPLY

AERONAUTICAL RESEARCH COUNCIL
REPORTS AND MEMORANDA

An Aerofoil Designed to give Laminar Flow over the Whole Surface with Boundary-Layer Suction

By
E. J. RICHARDS, M.A., B.Sc. and C. H. BURGE,
of the Aerodynamics Division, N.P.L.

LONDON : HIS MAJESTY'S STATIONERY OFFICE
1949
Price 2*s.* 6*d.* net

An Aerofoil Designed to give Laminar Flow over the Whole Surface with Boundary-Layer Suction

By
E. J. RICHARDS, M.A., B.Sc. and C. H. BURGE,
of the Aerodynamics Division, N.P.L.

Reports and Memoranda No. 2263
June, 1943

Summary.—A new type of aerofoil is described over the whole of which it is possible to maintain laminar flow by means of a small amount of boundary-layer suction. Preliminary small scale experiments at Reynolds numbers of about $0{\cdot}37 \times 10^6$ show that the mass flow it is necessary to remove by suction is less than that in the laminar boundary layer at the slot.

On the basis of these small-scale experiments the effective drag of this aerofoil at a Reynolds number R is estimated to be approximately $6{\cdot}0R^{-1/2}$. Thus at the Reynolds numbers reached in present day flight (say 25×10^6) an effective drag coefficient of 0·0012 may be expected. These figures are all subject to experimental confirmation at higher Reynolds numbers.

Further Investigation.—More elaborate tests are to be made in the National Physical Laboratory 13 ft. × 9 ft. wind tunnel at Reynolds numbers up to 5×10^6. Other experiments are also planned in the N.P L. Rectangular High-Speed Tunnel.

Introduction.—Experiments on boundary-layer control by suction have shown that no marked decrease in drag is obtainable on aerofoils of normal thickness over which separation does not occur. With abnormally thick profiles, a considerable improvement in drag has been observed but this is invariably due to the prevention of separation. To reduce the drag of a normal aerofoil, when there is an adverse velocity gradient over most of the chord, a series of slots or perforated sheets are necessary to maintain laminar flow over the whole chord and in order to obtain an efficient system, the suctions at each of these slots must differ. Consequently the internal ducting arrangement becomes very complicated and a prohibitive increase in structure weight occurs.

The present scheme, arising from a suggestion by Dr. A. A. Griffiths for improving the efficiencies of diffusers, consists of designing the aerofoil so that, according to potential flow theory, it has a stabilizing velocity gradient along the whole chord except at one position where a discontinuity of velocity occurs. Thus if sufficient suction is applied at this one point to prevent separation, laminar layers should persist right to the trailing edge. Apart from the greater simplicity of the suction system, this arrangement should result in a decrease in the drag of aerofoils of all thicknesses since it should prevent transition to turbulence as well as separation.

Design of Aerofoil.—A method is given in Ref. 1 for calculating the shape of the aerofoil profile which has (to a first approximation) any prescribed velocity distribution over its surface. If x denotes the distance along the chord from the leading edge and y the ordinate at that point both measured as fractions of the chord, the aerofoil profile for which the approximate velocity distribution is linear in each of two segments but discontinuous at the join $x = X_1$ has been calculated ; with the notation of Fig. 1, the ordinates of the aerofoil are given by

$$y = af_0 + bf_1 + df_2 + (b - c)f_3$$

where f_0, f_1 and f_2 have the same values as in section 6 of Ref. 1 and

$$f_3 = -\frac{1}{4\pi}(\cos\theta - \cos\theta_1)\left(2 + \frac{\cos\theta - \cos\theta_1}{1 + \cos\theta_1}\right)\log_e \frac{\sin\frac{1}{2}|\theta - \theta_1|}{\sin\frac{1}{2}(\theta + \theta_1)}$$

$$+ \frac{\sin\theta_1 - 2(\pi - \theta_1)}{4\pi(1 + \cos\theta_1)}\sin\theta - \frac{\pi - \theta_1}{8\pi(1 + \cos\theta_1)}\sin 2\theta$$

where

$$x = \tfrac{1}{2}(1 - \cos\theta),\ X_1 = \tfrac{1}{2}(1 - \cos\theta_1).$$

Formulae for the leading edge and trailing edge radii of curvature and expressions for functions necessary to obtain a closer approximation to the velocity distribution are given in the Appendix.

In choosing an aerofoil for test, X_1 was taken to be $0{\cdot}7$. This figure was chosen for structural reasons only since smaller values of X_1 gave aerofoils with a long sting (*see* Fig. 2*d* showing the aerofoil profile for $X_1 = 0{\cdot}5$, $a = 0{\cdot}268$, $b = 0{\cdot}308$, $c = -0{\cdot}092$, $d = -0{\cdot}052$).

When $X_1 = 0{\cdot}7$

$$f_3 = -\frac{1}{\pi}\left\{0{\cdot}5(\cos\theta + 0{\cdot}4) + 0{,}4166667(\cos\theta + 0{\cdot}4)^2\right\}$$

$$\times \log_e\left|\frac{1 + 0{\cdot}4\cos\theta - 0{\cdot}9165151\sin\theta}{0{\cdot}4 + \cos\theta}\right| - 0{\cdot}1859518\sin\theta - 0{\cdot}0768771\sin 2\theta$$

and is tabulated against x in Table 2.

From this table of f_3 in conjunction with tables of f_0, f_1 and f_2 for $X_1 = 0{\cdot}7$ in Ref. 1, the ordinates of the aerofoil are easily calculated for any values of a, b, c and d.

Since with suction a stagnation point must occur at the rear lip of the slot, it is desirable that the aerofoil should be designed to have a stagnation point there. It was found however that with a stagnation point ($c = -1$) the method of analysis does not lead to a simple closed contour, since the upper surface ordinates change sign towards the tail. The aerofoil finally decided upon for the tests was therefore designed to give a sharp decrease of velocity at the slot equal to half the free stream velocity ($b - c = 0{\cdot}5$). In the notation of Fig. 1, a first approximation to the velocity distribution over the aerofoil is derived by making $X_1 = 0{\cdot}7$, $a = 0{\cdot}1$, $b = 0{\cdot}3$, $c = -0{\cdot}2$, $d = -0{\cdot}05$. Tables of ordinates and of functions necessary to obtain a closer approximation to the velocity distribution over this section are given in Table 3. The aerofoil shape is shown in Fig. 2*a*. Close approximation to the potential flow velocity distribution for a range of lift coefficients are shown in Fig. 3.

The thickness-chord ratio of the aerofoil is $16{\cdot}3$ and its maximum thickness is at $0{\cdot}47$ chord. For these preliminary tests, the stabilising velocity gradient was designed to be greater than that of a normal low-drag aerofoil in order to allow a considerable tolerance in surface waviness.

Method of Analysis.—Consider the whole suction installation arranged inside the aerofoil, the air being discharged from the pump in the direction of the free stream with a velocity and pressure equal to that of the free stream. Neglecting any external drag the discharging system may have, the profile drag in this case, being the rate of loss of momentum in the direction of the free stream inside any large contour enveloping the aerofoil and discharge system over which the pressure may be assumed constant, is equal to that measured by pitot traverse across the wake when the air is removed elsewhere, since the sink drag is regained by the jet effect of the discharged air. To this, a term must be added to account for the power H used to drive the pumping mechanism. If D is the drag measured by pitot traverse across the wake, and V_0 is the free stream velocity, the effective drag will be $D + \frac{\eta H}{V_0}$ where η is the efficiency of the propulsive unit of the aircraft.

Without a knowledge of the actual ducting system, it is impossible to make an estimate of the power H which is extended in overcoming both the skin frictional drag of the aerofoil up to the slots and the internal frictional drag. Simple actuator disc theory is sufficient to give a rough measure of the effective drag in terms of the velocity and pressure inside the slot.

Suppose the velocity and pressure in the free-stream and at some point in the ducting system are (V_0, p_0) and (V_s, p_s) respectively. With the notation of the diagram and neglecting skin frictional losses aft of the measuring point inside the duct (with the notation of the diagram)

$$p_s + \tfrac{1}{2}\rho V_s^2 = p_f + \tfrac{1}{2}\rho V_f^2$$

$$p_0^2 + \tfrac{1}{2}\rho V_0^2 = p_f + \Delta p_f + \tfrac{1}{2}\rho V_f^2$$

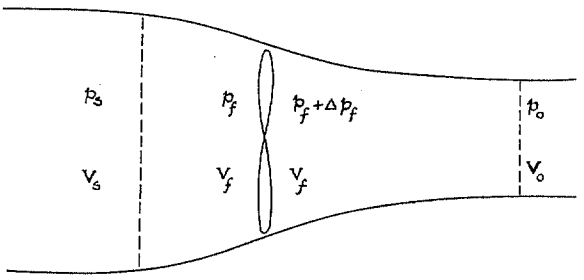

Thus the pressure difference across the fan disc is

$$\Delta p_f = (p_0 - p_s) + \tfrac{1}{2}\rho\,(V_0^2 - V_s^2).$$

The energy imparted into the air in unit time is

$$\Delta p_f \times Q$$

where Q is the volume of air passing the fan in unit time and

$$\frac{H}{V_0} = \frac{Q.\Delta p_f}{R\,V_0}$$

if R is the efficiency of the pump. If non-dimensional coefficients C_p, C_Q are defined by $C_p = \frac{p_0 - p_s}{\frac{1}{2}\rho V_0^2}$ and $C_Q = \frac{Q}{CV_0}$ where c = aerofoil chord, then the effective drag coefficient

$$C_D' = C_D + \frac{\eta}{R}\left[C_p\,C_Q + C_Q\left(1 - \frac{V_s^2}{V_0^2}\right)\right]. \quad .. \quad .. \quad .. \quad .. \quad (1)$$

If it is assumed that the efficiency of the suction pump is equal to that of the main propulsion unit of the aircraft, R should be taken equal to η ; hence

$$C_D' = C_D + C_Q\left(1 - \frac{V_s^2}{V_0}\right) + C_Q\,C_p\,.$$

It should be made clear that this expression does not give the drag coefficient likely to occur in flight but gives a rough method of interpreting wind-tunnel results to include the energy of the pump and the entry losses. The duct losses aft of the position where p_s is measured as well as the external drag of the discharge system are neglected in this analysis. However, the wind-tunnel experiments are made with the air being brought to rest in a large chamber in such a way that it loses all its kinetic energy, and since the above expression includes this loss, the " effective " drag coefficient obtained is not considered too optimistic.

Experimental.—A small model of 18 inches chord was tested in a 4-ft. wind tunnel of fairly low turbulence. The aerofoil (Fig. 2*a*) was made in two sections, the rear section being made of tufnol* to avoid breakage or distortion. Suction was applied at slots of 0·1 inch width on both surfaces at the joint between the two sections (0·7 chord). In order to maintain a uniform suction along the whole span, the suction cavity was divided into two chambers, separated by gauzes, the air being taken away at each end of the span of the inner chamber. The quantity of air absorbed was measured by means of a calibrated nozzle in the duct leading to the suction pump, while the static pressure inside the chamber was measured by shielded static holes in the cavity itself. The velocity there was small and was neglected.

* A proprietary make of laminated plastic material.

In later experiments the model was modified to incorporate additional slots of 0·6 inches width at 0·65 chord. The form of the suction chambers with the two slots in each surface is shown in Fig. 2*b*.

The rear slot width could be modified by chordwise movements of the tail piece of the aerofoil relative to the main structure. The slight change in aerofoil shape did not alter the velocity distribution sufficiently to affect the results. A range of slot widths was investigated covering from half to twice the thickness of the calculated laminar boundary-layer thickness δ at 0·7 of the chord. This was calculated from the formula of Ref. 2.

$$R\,(Q/c)^2 = \frac{0\cdot470}{S^{6\cdot28}} \int_0^{x/c} S^{5\cdot28}\ \ d\,(x/c)$$

and

$$\delta = 8\cdot51\,\theta.$$

where S is the ratio of the local velocity over the surface to that of the free stream.

Description of the Experiments.—Preliminary experiments were made with suction applied along the whole span at 0·7 of the chord. As the maximum suction available was insufficient to induce laminar flow over the tail, the span over which suction was applied was reduced to half a chord. In view of the tentative nature of these experiments, a section off the centre of the span was used, no end plates being fitted and no readings of internal pressure being taken.

In order to obtain a picture of the exact nature of the air flow over the aerofoil, wood smoke[3] was emitted from three small slots, slightly staggered spanwise, one at 0·1 chord from the leading edge and the others on the tail piece at 0·73 and 0·83 of the chord. By emitting thin filaments of dense smoke from these slots a clear conception of the position and nature of transition and separation was obtained.

With suction applied to this small spanwise section, laminar flow over the whole span could be induced, but the mass flow into the slot amounted to over ten times the air in the laminar boundary layer at 0·7 chord. Actual pitot-traverse measurements in the wake gave a drag coefficient, which when based on the rear part of the chord (0·3*c*) lay between that of the laminar and turbulent drag of a flat plate. It was at once apparent that, at the Reynolds number of this test ($R = 2\cdot4 \times 10^5$), laminar separation occurred at 0·55 — 0·60 chord in the absence of suction, so that a considerable sink effect was necessary at 0·7 chord to modify the pressure distribution as far forward as 0·55 chord. No noticeable reduction in suction was obtainable by first increasing the suction to establish the flow and then reducing the suction slowly.

Consequently an additional slot was cut at 0·65 chord and the internal arrangement modified so that the suction head at each slot could be controlled independently. After a considerable amount of modification to the slot width and entry shape, laminar flow was maintained over the whole chord by removing from each surface by suction one half of the calculated amount of air in the laminar boundary layer at 0·7 chord. It should be made clear however that no end plates were fitted in this case.

Pressure Plotting Experiments.—At this stage the experiments were continued with the test section at the centre of the span; end plates were fitted to eliminate cross-flow effects and the internal arrangement again modified (Fig. 2*c*). In order to investigate the unexpectedly far forward position of laminar separation, pressure holes were fitted in the surface. Pressures up to 0·7 chord were measured by copper tubes sunk along the surface, the final surface with these in position being good except between the front and rear slots. Pressures over the tail were obtained by drilling a cavity inside the tufnol and leading fine holes from it to the required position on the surface.

Fig. 4 shows a comparison of the velocity distribution over the surface without suction, and with sufficient suction to allow laminar flow over the tail of the aerofoil; the experimental

pressures are corrected to free air conditions by using the known correction on a Rankine oval having the same chord and maximum thickness[4]. Without suction, the discrepancy of 1 per cent. between theory and experiment over the front third of the aerofoil cannot be accounted for by interference of end plates, effect of boundary layer thickness, or inaccuracy in the surface.

The velocity gradient over the first half of the chord is approximately equal to that of theory ; after this, however, a gradual decrease of velocity occurs which accounts for the early laminar separation observed in the smoke experiments. The slight hump between the slots may be accounted for by poor surface condition at the pressure holes.

The velocity distribution when sufficient suction is applied to allow laminar flow over the trailing edge (Fig. 4) indicates a general increase in velocity over the front of the aerofoil. This is not unexpected since this effect may be noticed on the potential flow velocities over a series of aerofoils with increasing concavity near the trailing edge. At the tail of the aerofoil, the theoretical velocities are not attained, although they are more closely approached if the suction is still further increased.

It was suggested by Mr. H. B. Squire that a turbulence wire should be put slightly forward of the position of laminar separation to cause transition to turbulence and consequently to delay separation. A steel wire of 0·028 inch diameter was placed at 0·55 chord and the pressure plotting and suction experiments were repeated. Some deficiency was experienced in observation to the rear of the wire, since the very fine smoke filaments could not be obtained in this condition. It appeared however that the boundary layer over the tail was in every case turbulent with the wire in position. Without suction, separation could be detected although not so clearly as before. Tests with suction through the back slot alone showed that to prevent a separation a much smaller quantity of air was necessary than without a wire present. Exact figures were difficult to obtain and perhaps a better indication is given by comparison of the pressure distributions with and without wires, under the same conditions of suction shown in Figs. 5 and 4 respectively. With turbulence wires the most noticeable features without suction are the slight backward movements of the positions of maximum velocity and the improved flow over the rear of the aerofoil. It would appear from this that the potential flow velocity distribution is likely to be more closely approximated at Reynolds numbers for which laminar separation is delayed further along the chord.

No attempt was made to improve the efficiency of the slots in these latter experiments. It was necessary in this case to suck away 0·7 of the volume of air calculated to be in the laminar boundary layer at 0·7 chord to maintain laminar flow over the whole aerofoil.

Effective Drag Coefficient.—The static pressure inside each cavity is shown in Fig. 4 and Fig. 5 In most cases this was found to be approximately equal to the static pressure on the forward lip of the slot ; since the velocity in the cavity was small, it follows that the intaken air lost all its kinetic energy in entering the cavity. If therefore in equation (1), $V_s = 0$ and $p_s =$ pressure in the cavity, the effective drag coefficients calculated will give a pessimistic estimate of that using a good ducting system since the large loss in the cavity will easily outweigh the duct losses on the outlet side of the pump.

Thus $C_D' = C_D + C_Q^* (1 + C_p)$.

For the experiments with end plates in position ($R = 3{\cdot}77 \times 10^5$) and taking the value of C_p for that slot (front) which would give the greater value of the effective drag, $C_Q = 0{\cdot}0041$ and $C_p = 0{\cdot}75$ so that

$$C_D' - C_D = 0{\cdot}0072.$$

C_D is the measured drag coefficient obtained by pitot traverse of the wake ; if this consists only of the profile drag of the aerofoil to the rear of the slot (which of course is not true if much less than the boundary layer is absorbed) C_D may be estimated with sufficient accuracy for the present purpose as being that of a flat plate of $0{\cdot}3c$ length and is equal to $2{\cdot}66R^{-1/2}\left(1 - \frac{x}{c}\right)^{1/2}$ (Ref. 5) where in this case $x = 0{\cdot}7c$.

Therefore $C_D = 1 \cdot 455 R^{-1/2} = 0 \cdot 00237$

when $R = 3 \cdot 77 \times 10^5$.

Thus the total effective drag coefficient $C_D' = 0 \cdot 0096$ at $R = 3 \cdot 77 \times 10^5$. The amount of air removed by suction in this case is equivalent to $0 \cdot 7$ times the quantity in the boundary layer. Since however the mean velocity of the outer $0 \cdot 3$ of the boundary layer will not differ greatly from that of the free stream, it is considered that the above figure is a conservative estimate of that occurring in practice.

The Effect of Reynolds Number.—At the Reynolds number of the tests, little if any reduction in drag coefficient is obtained by boundary-layer suction. If, however, the reasonable assumption is made that the same proportion of the boundary layer must be absorbed at all Reynolds numbers and that the pressure coefficient C_p is unaltered, considerable reductions in drag coefficient are possible at higher values of R.

The calculated laminar boundary-layer thickness (δ) at $0 \cdot 7$ chord for this aerofoil is given by

$$\delta/c = 2 \cdot 44/R^{1/2}.$$

C_Q therefore varies with $R^{-1/2}$ and, in order to satisfy the experimental figures, etc. $R = 3 \cdot 77 \times 10^5$, must take the form $C_Q = 2 \cdot 52 \times R^{-1/2}$. Thus the effective drag coefficient $= 1 \cdot 46 R^{-1/2} + 4 \cdot 41 R^{-1/2} = 6 \cdot 07 R^{-1/2}$.

The following Table shows the variation of C_Q, $C_Q\ (1 + C_p)$, C_D and the effective drag coefficient C_D' with Reynolds number.

TABLE 1

R	C_Q	$C_Q\ (1 + C_p)$	C_D	C_D'
10^5	0·00796	0·01393	0·00460	0·01853
10^6	0·00252	0·00441	0·00145	0·00586
10^7	0·00079	0·00139	0·00046	0·00185
10^8	0·00025	0·00044	0·00014	0·00059

Fig. 6 gives a comparison for varying Reynolds numbers of the drag coefficients of several modern low-drag aerofoils[6,7,8] and that estimated for the suction aerofoil under consideration. Whereas the effective drag coefficient obtained in the present tests is approximately equal to those of ordinary low-drag aerofoils at the same Reynolds number, a considerable reduction may be expected at Reynolds numbers such as those reached in present-day flight.

Discussion.—Variations of slot width and entry conditions are not given in the present report since it is considered that such information will be in error and misleading at Reynolds numbers for which the scheme gives reduced effective drag. At these flight conditions, the early laminar separation may not occur and it is possible that a single suction slot at $0 \cdot 7$ chord will be efficient under these conditions. Sufficient results have been presented however to give experimental verifications of the theory underlying the scheme and to show that in fact less air must be sucked away than that in the laminar boundary layers at the slot.

Further tests are to be made on the same aerofoil profile in a wind tunnel of low turbulence at Reynolds numbers up to 5×10^6 to confirm the present results and to investigate fully the question of slot width and shape of entry.

Conclusions.—(1) Laminar flow over the whole of the chord of an aerofoil is possible by a suitable design of aerofoil and by boundary-layer suction at either one or two positions along the chord.

(2) Preliminary experiments at $R = 3{\cdot}8 \times 10^5$ show that the amount of boundary layer air that must be removed by suction is less than that calculated to be in the laminar boundary layer at the slot.

(3) Owing to the forward position of laminar separation on the aerofoil at the Reynolds numbers of the tests, two slots were necessary on each surface to reduce the suction air to that stated in (2) one being $0{\cdot}05$ chord ahead of the calculated position.

(4) The effective drag coefficient of the aerofoil at zero incidence assuming pessimistic duct conditions, may be put in the form $6{\cdot}0 \times R^{-1/2}$ and is approximately equal to that of a normal low-drag aerofoil at $R = 3{\cdot}7 \times 10^5$. Extrapolation to higher Reynolds numbers indicates however that a considerable reduction of drag is possible at the conditions of present-day flight.

APPENDIX

Useful Functions Relating to the Suction Aerofoil

The expressions given below have been calculated by the method of Ref. 1 for an aerofoil over which the velocity distribution (to a first approximation) is linear in each of two segments of the chord but discontinuous at the join.

Using the notation of Fig. 1, the leading edge and trailing edge radii of curvature are given by

$$
\begin{aligned}
(2\rho_L)^{1/2} = {} & \frac{a}{2\pi\,(1-\cos\theta_1)}\left\{2\sin\theta_1 - 2\,\theta_1\cos\theta_1 + \theta_1 - \sin\theta_1\cos\theta_1\right\} \\
& + \frac{b}{1+\cos\theta_1}\left\{\frac{3}{2} - \frac{1}{\pi\,(1-\cos\theta_1)}\right. \\
& \left.\times\,(2\sin\theta_1 - 2\theta_1\cos\theta_1 + 0_1 - \sin\theta_1\cos\theta_1)\right\} \\
& + \frac{d}{1+\cos\theta_1}\left\{\frac{1}{2\pi}\,(2\sin\theta_1 - 2\theta_1\cos\theta_1 + \theta_1 - \sin\theta_1\cos\theta_1) - \tfrac{1}{2} + \cos\theta_1\right\} \\
& + \frac{b-c}{1+\cos\theta_1}\left\{\frac{1}{2\pi}\,(4\sin\theta_1 + 3\,\theta_1 + \sin\theta_1\cos\theta_1) - \frac{3}{2}\right\}
\end{aligned}
$$

$$
\begin{aligned}
(2\rho_T)^{1/2} = {} & \frac{a}{2\pi\,(1-\cos\theta_1)}\left\{(2\sin\theta_1 - 2\,\theta_1\cos\theta_1 - \theta_1 + \sin\theta_1\cos\theta_1)\right\} \\
& + \frac{b}{1+\cos\theta_1}\left\{\tfrac{1}{2} - \frac{1}{\pi\,(1-\cos\theta_1)}\,(2\sin\theta_1 - 2\theta_1\cos\theta_1 - \theta_1 + \sin\theta_1\cos\theta_1)\right\} \\
& + \frac{d}{(1+\cos\theta_1)}\left\{\tfrac{1}{2} + \cos\theta_1 + \frac{1}{2\pi}\,(2\sin\theta_1 - 2\,\theta_1\cos\theta_1 - \theta_1 + \sin\theta_1\cos\theta_1)\right\} \\
& + \frac{b-c}{1+\cos\theta_1}\left\{\frac{1}{2\pi}\,(\theta_1 - \sin\theta_1\,\cos\theta_1) - \tfrac{1}{2}\right\}
\end{aligned}
$$

In determining a closer approximation to the velocity distribution, the functions C_0, ε_s and ε_s' defined in Ref. 1 are required. For convenience these are given below.

$$C_0 = \frac{a\,(1-\cos\theta_1)}{4} + \frac{b}{2} + d\,\frac{1+\cos\theta_1}{4} - (b-c)\,\frac{1+\cos\theta_1}{4}$$

$$\varepsilon_s = \tan\tfrac{1}{2}\theta\left\{\frac{(b-a)\,(\cos\theta_1-\cos\theta)}{2\,(1-\cos\theta_1)} + \frac{(a-d)}{4}\,(1+\cos\theta_1) + \frac{b-c}{4}\,(1+\cos\theta_1)\right\};\quad 0 \leqslant \theta \leqslant \theta_1$$

$$= \cos \tfrac{1}{2}\theta \left\{ \frac{(c-d)(\cos\theta_1 - \cos\theta)}{2(1+\cos\theta_1)} + \frac{a-d}{4}(1-\cos\theta_1) + \frac{b-c}{4}(1-\cos\theta_1) \right\} \; ; \; \theta_1 \leqslant \theta \leqslant \pi .$$

$$\varepsilon_s' = \frac{1+\cos\theta_1}{1+\cos\theta}\left\{ \frac{b}{2(1-\cos\theta_1)} - \frac{a(1+\cos\theta_1)}{4(1+\cos\theta_1)} - \frac{d}{4} + \frac{b-c}{4} \right\} - \frac{b-a}{2(1-\cos\theta_1)}\cos\theta \; ; \; 0 < \theta_1 \leqslant \theta_1$$

$$= \frac{1-\cos\theta_1}{1-\cos\theta}\left\{ \frac{c}{2(1+\cos\theta_1)} - \frac{a}{4} - \frac{d(1-\cos\theta_1)}{4(1+\cos\theta_1)} - \frac{b-c}{4} \right\} + \frac{c-d}{2(1+\cos\theta_1)}\cos\theta \; ; \; \theta_1 \leqslant \theta \leqslant \pi .$$

There is a discontinuity in ε_s' at $\theta = \theta_1$.

$$\varepsilon_s'(\theta_1 - 0) = \frac{3b - a - c - d}{4}$$

$$\varepsilon_s'(\theta + 0) = \varepsilon_s'(\theta - 0) - (b - c) .$$

When $X_1 = 0{\cdot}7$

$$\cos\theta_1 = -0{\cdot}4 \quad \theta_1 = 1{\cdot}9823132 \quad \sin\theta_1 = 0{\cdot}9165151$$

$$(2\rho_L)^{1/2} = 0{\cdot}6556956a + 0{\cdot}2670301b + 0{\cdot}0473178c + 0{\cdot}0299565d$$

$$(2\rho_T)^{1/2} = 0{\cdot}1216355a + 0{\cdot}2176184b + 0{\cdot}2102632c + 0{\cdot}4504828d$$

$$C_0 = 0{\cdot}35(a+b) + 0{\cdot}15(c+d)$$

$$\varepsilon_s = \tan\tfrac{1}{2}\theta\{0{\cdot}2928571a + 0{\cdot}0071429b - 0{\cdot}15c - 0{\cdot}15d - 0{\cdot}3571429(b-a)\cos\theta\} \quad \text{for } 0 \leqslant x \leqslant 0{\cdot}7$$

$$= \cot\tfrac{1}{2}\theta\{0{\cdot}35a + 0{\cdot}35b - 0{\cdot}6833333c - 0{\cdot}166667d - 0{\cdot}8333333(c-d)\cos\theta\} \quad \text{for } 0{\cdot}7 \leqslant \theta_1 \leqslant 1$$

$$\varepsilon_s' = \frac{1}{1+\cos\theta}\{0{\cdot}3642857b - 0{\cdot}0642857a - 0{\cdot}15c - 0{\cdot}15d\} - 0{\cdot}3571429(b-a)\cos\theta\} \quad \text{for } 0 \leqslant x \leqslant 0{\cdot}1$$

$$= \frac{1}{1-\cos\theta}\{1{\cdot}5166667c - 0{\cdot}35a - 0{\cdot}35b - 0{\cdot}8166667d\} + 0{\cdot}8333333(c-d)\cos\theta\} \quad \text{for } 0{\cdot}7 \leqslant x \leqslant 1.$$

When $X_1 = 0{\cdot}7$, $a = 0{\cdot}1$, $b = 0{\cdot}3$, $c = -0{\cdot}2$, $d = -0{\cdot}05$

$$\rho_L = 0{\cdot}0090744, \quad \rho_T = 0{\cdot}0000828$$

$$C_0 = 0{\cdot}1025$$

$$\varepsilon_s = \tan\tfrac{1}{2}\theta \; \{0{\cdot}0689286 - 0{\cdot}0714286\cos\theta\} \quad \text{for } 0 \leqslant x \leqslant 0{\cdot}7$$

$$= \cos\tfrac{1}{2}\theta \; \{0{\cdot}2775 + 0{\cdot}125\cos\theta\} \quad \text{for } 0{\cdot}7 \leqslant x \leqslant 1.$$

$$\varepsilon_s' = \frac{0{\cdot}1403571}{1+\cos\theta} - 0{\cdot}0714286\cos\theta \quad \text{for } 0 \leqslant x \leqslant 0{\cdot}7.$$

$$= -\frac{0{\cdot}4025}{(1-\cos\theta)} - 0{\cdot}125\cos\theta \quad \text{for } 0{\cdot}7 \leqslant x \leqslant 1.$$

REFERENCES

No.	Author	Title, etc.
1	Goldstein, S. and Richards, E. J. ..	A Theory of Aerofoils of Small Thickness. Part III. Approximate Designs of Symmetrical Aerofoils for Specified Pressure Distributions. A.R.C. 6225. October, 1942. (To be published.)
2	Young, A. D. and Winterbottom, N. E.	Note on the Effect of Compressibility on the Profile Drag of Aerofoils at Subsonic Mach Numbers in the Absence of Shock Waves. R. & M. 2400. May, 1940.
3	Preston, J. H. and Sweeting, N. E. ..	Wood Smoke as a means of Visualising Boundary Layer Flow at High Reynolds Numbers. *J. Roy. Ae. Soc.* Vol. XLVII. No. 387. March, 1943. Also A.R.C. 5537.
4	Fage, A., Stanton, T. E. and Glauert, H.	On the Two-dimensional Flow Past a Body of Symmetrical Cross-section mounted in a Channel of Finite Breadth. R. & M. 1223. February, 1929.
5	Goldstein, S. (Editor)	Modern Developments in Fluid Dynamics. p. 136. Oxford Clarendon Press. 1938.
6	Ellis, M. C. Jr.	Some Lift and Drag Measurements of a Representative Bomber Nacelle on a Low-drag Wing—II. N.A.C.A. Confidential Bulletin. September, 1942. A.R.C. 6434.
7	Staff of the Compressed Air Tunnel, N.P.L.	Tests in the Compressed Air Tunnel of Four Aerofoils having their Maximum Thickness at 50 per cent. of the Chord. A.R.C. 4978. February, 1941. (Unpublished.)
8	Winterbottom, N. E. and Squire, H. B.	Note on the Further Wing Profile Drag Calculations. R.A.E. Report B.A. 1634. A.R.C. 4871. October, 1940. (Unpublished.)
9	Squire, H. B. and Young, A. D. ..	The Calculation of the Profile Drag of Aerofoils. R. & M. 1838. November, 1937.

TABLE 2

$x_1 = 0{\cdot}7$

x/c	$f_3(\theta)$
0	0
0·005	−0·0033560
0·0075	−0·0041163
0·0125	−0·0053300
0·025	−0·0075955
0·050	−0·0109103
0·075	−0·0135789
0·100	−0·0159425
0·150	−0·0202220
0·200	−0·0242487
0·250	−0·0282431
0·300	−0·0323520
0·350	−0·0367066
0·400	−0·0414525
0·450	−0·0467777
0·500	−0·0529578
0·550	−0·0604453
0·600	−0·0700994
0·650	−0·0839933
0·700	−0·1140605
0·750	−0·1348540
0·800	−0·1282862
0·850	−0·1104399
0·900	−0·0854404
0·950	−0·0547109
1·000	0

TABLE 3

$X_1 = 0{\cdot}7$

$a = 0{\cdot}1,\ b = 0{\cdot}3,\ c = -0{\cdot}2,\ d = -0{\cdot}05,\ C_0 = 0{\cdot}1025$

x/c	y/c	ψ_s	ε_s	ε_s'
0	0		0	0
0·005	0·00954	0·13523	−0·00013	−0·00018
0·0075	0·01169	0·13549	−0·00012	+0·00035
0·0125	0·01511	0·13600	−0·00008	0·00142
0·025	0·02143	0·13727	+0·00017	0·00412
0·050	0·03046	0·13976	0·00107	0·00959
0·075	0·03745	0·14219	0·00234	0·01515
0·100	0·04337	0·14455	0·00393	0·02083
0·150	0·05322	0·14904	0·00795	0·03256
0·200	0·06126	0·15315	0·01304	0·04487
0·250	0·06790	0·15681	0·01918	0·05786
0·300	0·07327	0·15989	0·02642	0·07168
0·350	0·07739	0·16225	0·03486	0·08654
0·400	0·08018	0·16366	0·04462	0·10268
0·450	0·08149	0·16381	0·05589	0·12046
0·500	0·08109	0·16219	0·06893	0·14036
0·550	0·07859	0·15797	0·08410	0·16310
0·600	0·07331	0·14965	0·10192	0·18973
0·650	0·06383	0·13383	0·12314	0·22194
0·700	0·04337	0·09464	0·14893	+0·26250
0·750	0·02314	0·05343	0·12413	−0·23750 −0·20583
0·800	0·01384	0·03461	0·10125	−0·17656
0·850	0·00840	0·02351	0·07982	−0·14926
0·900	0·00512	0·01705	0·05917	−0·12361
0·950	0·00300	0·01379	0·03785	−0·09934
1·000	0	0	0	−0·07625

ε' is discontinuous at the slot.

(85746) B

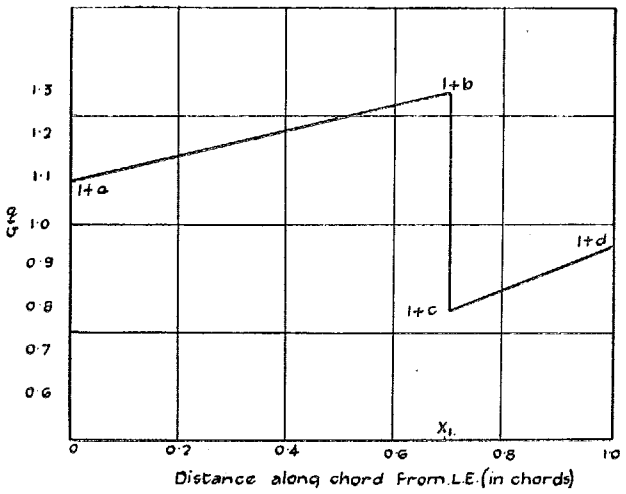

FIG. 1. Assumed Velocity Distribution over Aerofoil.

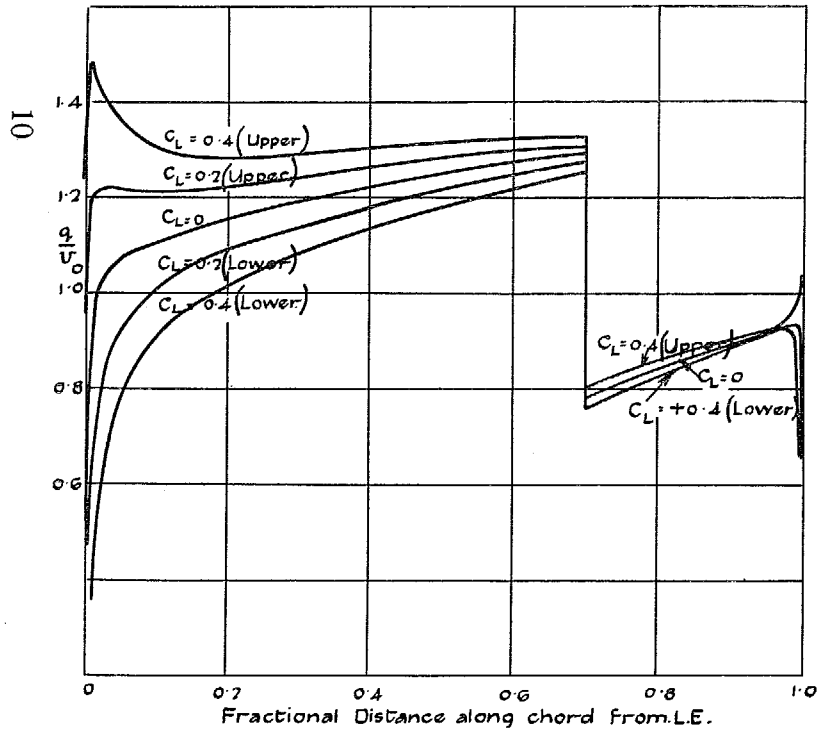

FIG. 3. Approximate Velocity Distribution over Aerofoil (Theoretical).
(Approx. III Ref. 1. Slope of lift curves = 2π.)

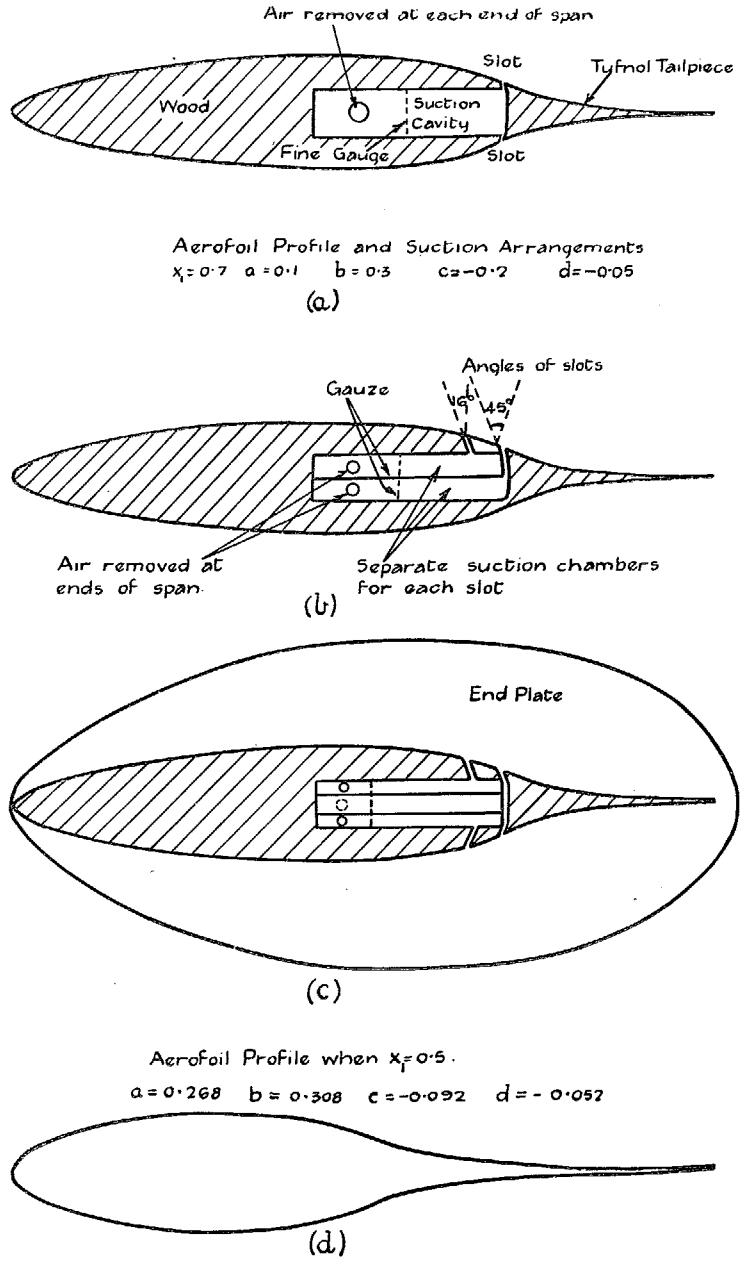

FIG. 2.

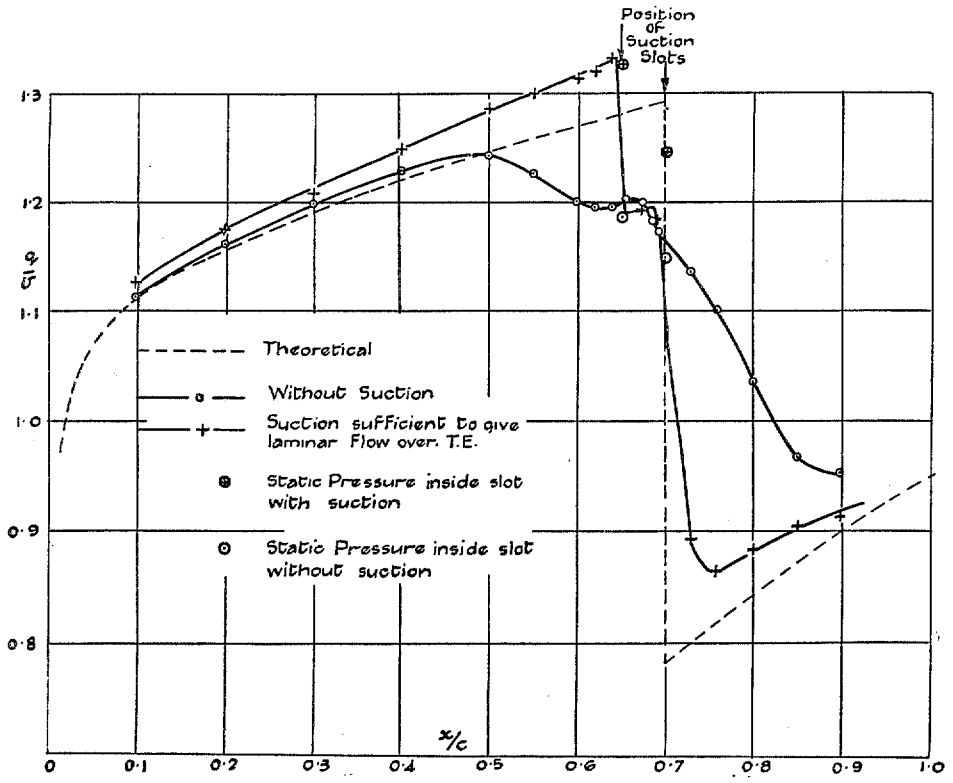

FIG. 4. Velocity Distribution over Aerofoil. Zero Incidence.

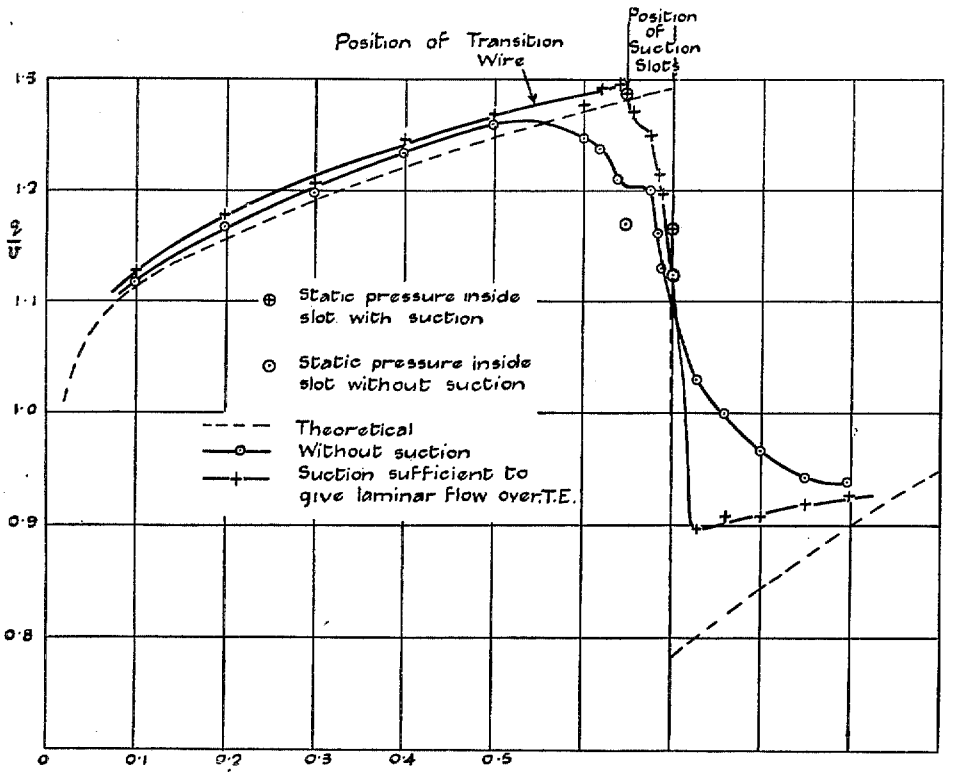

FIG. 5. Velocity Distribution over Aerofoil. Zero Incidence. Transition Wire at 0·55*c*.

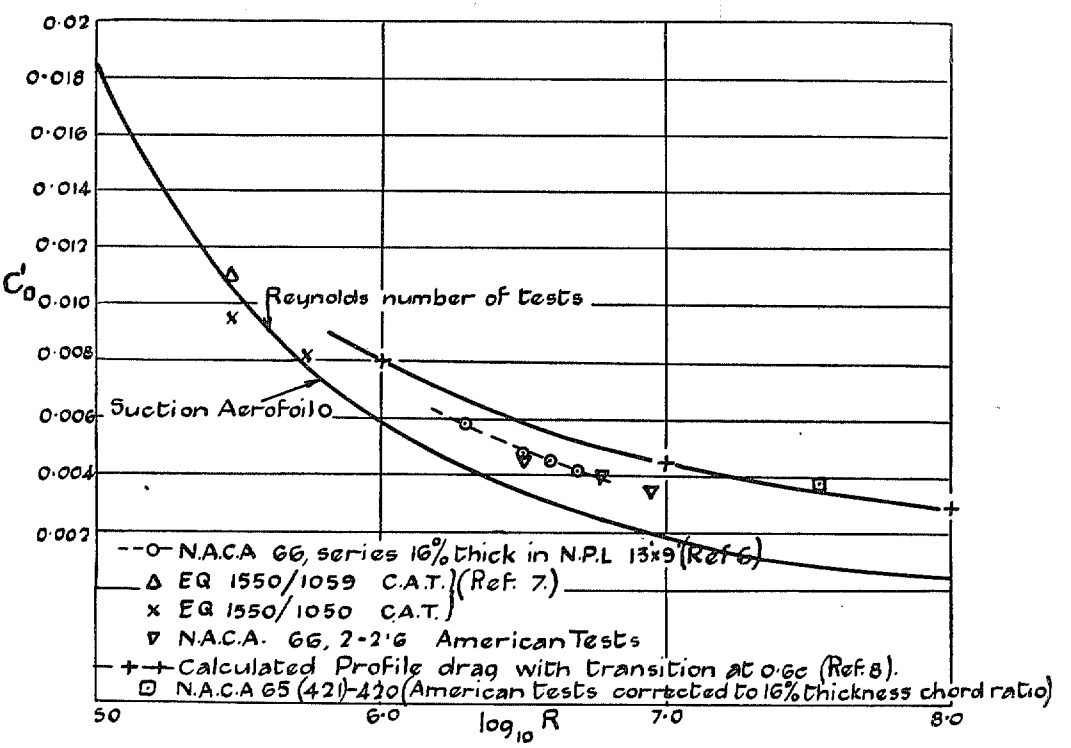

FIG. 6. Comparison of Effective Drag of Suction Aerofoil.

(85746) Wt. 12/818 8/49 Hw.

PRINTED IN GREAT BRITAIN

Publications of the Aeronautical Research Committee

TECHNICAL REPORTS OF THE AERONAUTICAL RESEARCH COMMITTEE—

1934–35 Vol. I. Aerodynamics. 40*s.* (40*s.* 8*d.*)
Vol. II. Seaplanes, Structures, Engines, Materials, etc. 40*s.* (40*s.* 8*d.*)
1935–36 Vol. I. Aerodynamics. 30*s.* (30*s.* 7*d.*)
Vol. II. Structures, Flutter, Engines, Seaplanes, etc. 30*s.* (30*s.* 7*d.*)
1936 Vol. I. Aerodynamics General, Performance, Airscrews, Flutter and Spinning. 40*s.* (40*s.* 9*d.*)
Vol. II. Stability and Control, Structures, Seaplanes, Engines, etc. 50*s.* (50*s.* 10*d.*)
1937 Vol. I. Aerodynamics General, Performance, Airscrews, Flutter and Spinning. 40*s.* (40*s.* 9*d.*)
Vol. II. Stability and Control, Structures, Seaplanes, Engines, etc. 60*s.* (61*s.*)
1938 Vol. I. Aerodynamics General, Performance, Airscrews, 50*s.* (51*s.*)
Vol. II. Stability and Control, Flutter, Structures, Seaplanes, Wind Tunnels, Materials. 30*s.* (30*s.* 9*d.*)

ANNUAL REPORTS OF THE AERONAUTICAL RESEARCH COMMITTEE—

1933–34 1*s.* 6*d.* (1*s.* 8*d.*)
1934–35 1*s.* 6*d.* (1*s.* 8*d.*)
April 1, 1935 to December 31, 1936. 4*s.* (4*s.* 4*d.*)
1937 2*s.* (2*s.* 2*d.*)
1938 1*s.* 6*d.* (1*s.* 8*d.*)

INDEXES TO THE TECHNICAL REPORTS OF THE ADVISORY COMMITTEE ON AERONAUTICS—

December 1, 1936 — June 30, 1939. R. & M. No. 1850. 1*s.* 3*d.* (1*s.* 5*d.*)
July 1, 1939 — June 30, 1945. R. & M. No. 1950. 1*s.* (1*s.* 2*d.*)
July 1, 1945 — June 30, 1946. R. & M. No. 2050. 1*s.* (1*s.* 1*d.*)
July 1, 1946 — December 31, 1946. R. & M. No. 2150. 1*s.* 3*d.* (1*s.* 4*d.*)
January 1, 1947 — June 30, 1947. R. & M. No. 2250. 1*s.* 3*d.* (1*s.* 4*d.*)

Prices in brackets include postage.

Obtainable from

His Majesty's Stationery Office

London W.C.2 : York House, Kingsway
[Post Orders—P.O. Box No. 569, London, S.E.1.]
Edinburgh 2 : 13A Castle Street
Birmingham 3 : 2 Edmund Street
Bristol 1 : Tower Lane
Manchester 2 : 39 King Street
Cardiff : 1 St. Andrew's Crescent
Belfast : 80 Chichester Street
or through any bookseller.